IEEE Access
Multidisciplinary ⋮ Rapid Review ⋮ Open Access Journal

Received December 11, 2019, accepted December 23, 2019, date of publication December 26, 2019,
date of current version January 6, 2020.

Digital Object Identifier 10.1109/ACCESS.2019.2962534

Robust Trajectory and Communication Design for Multi-UAV Enabled Wireless Networks in the Presence of Jammers

YANG WU[1], WENLU FAN[2], WEIWEI YANG[1], XIAOLI SUN[1], AND XINRONG GUAN[1]
[1]College of Communication Engineering, Army Engineering University of PLA, Nanjing 210007, China
[2]Business School, Nanjing University, Nanjing 210008, China

Corresponding author: Wenlu Fan (fwl19970204@126.com)

This work was supported by the National Natural Science Foundation of China under Grant 61471393 and 61771487.

ABSTRACT This paper investigates a multi-unmanned aerial vehicle (UAV) enabled wireless communication, where a number of ground nodes (GNs) are scheduled to communicate with UAVs in the presence of jammers with imperfect location information. Considering different quality of service (QoS) requirements for a wide range of applications, we aim to improve the minimum throughput, the average throughput, and the delay-constrained minimum throughput of all GNs, respectively, via the joint design of UAVs' trajectories, GNs' scheduling and power allocation. However, the formulated optimization problems are difficult to solve due to the non-convex and combinatorial nature. To overcome this difficulty, we propose two block coordinate descent (BCD) based algorithms to solve them sub-optimally with the aid of slack variables, successive convex approximation (SCA) technique and S-procedure. Numerical results show that our proposed algorithms outperforms the benchmark algorithms and offers a considerable gain in the view of different QoS requirements, giving a certain practical significance.

INDEX TERMS UAV communications, trajectory optimization, anti-jamming, robust design, QoS requirement.

I. INTRODUCTION

With the advantages such as wide coverage, on-demand deployment and line-of-sight (LoS) channels, unmanned aerial vehicles (UAVs) have attracted increasing attention in numerous applications such as remote surveillance, photography, agricultural irrigation, traffic control, cargo transportation and telecommunications, etc [1]–[3]. To support the various usages of UAV, wireless communication is of great significance. Because in any UAV-enabled application, either the UAV's control and non-payload communication (CNPC) to ensure reliable and safe flight mission or the payload communication relating specific missions need to be guaranteed.

Specifically, with the fully controllable UAV mobility, the communication distance between the UAV and the ground nodes (GNs) can be significantly shortened by proper trajectory design, thus improving the performance of the UAV-enabled wireless communication system. Motivated by this, extensive efforts have been done by properly designing the trajectory of UAV [4]–[7]. In [4], the minimum throughput of all GNs was enhanced via joint trajectory and transmit power optimization. In [5], the sum throughput of all GNs was improved by joint trajectory, transmit power and bandwidth optimization subject to the propulsion energy constraint. In [6], the UAV-enabled mobile relaying communication system was investigated, wherein the throughput of the source GN to the destination GN was optimized. In [7], the energy-efficiency of the UAV was studied, wherein the tradeoff between propulsion energy and throughput was derived.

However, the broadcasting nature of radio propagation makes the wireless communication particularly vulnerable to security threats, e.g., eavesdropping and jamming. To combat eavesdropping attacks, physical layer security (PLS) has been widely studied in the terrestrial networks [8]–[15], and recently, plenty of works have been done for UAV communications with the UAV's trajectory design and communication resources allocation. In [16], a UAV-enabled wireless network consists of a source UAV node, a destination GN and a eavesdropper GN was investigated, wherein the secrecy throughput was enhanced via joint trajectory and

The associate editor coordinating the review of this manuscript and approving it for publication was Xujie Li.

power allocation optimization. In [17], a dedicated UAV was deployed as a friendly jammer to degrade the reception of the eavesdropper and thus to enhance the secrecy performance. In [18], the UAV-relayed wireless networks with caching was introduced. In [19] and [20], the secrecy energy efficiency was considered, where the UAVs were regarded as a user and a relay, respectively.

Nevertheless, most of the works concerning PLS in UAV communication assume that the attackers' location is perfectly known, which is impractical for most application scenarios. In [21] and [22], the eavesdropper's location information was partially known, the lower bound of the secrecy rate was derived to evaluate the worst case performance and the UAV's trajectory and resource allocation were jointly optimized. In [23] and [24], the impacts of uncertain location of eavesdroppers was properly tackled via a robust algorithm so that the secrecy performance was significantly improved.

Meanwhile, extensive works have been done to combat jamming attacks in UAV-enabled communication [25]–[30]. In [25], a UAV was statically deployed to relay the message against a jammer. In [26], by formulating the competitive relations between the UAV and the jammer, a position strategy of the UAV was proposed to enhance the system performance. However, without providing sequential trajectory, [25] and [26] explored little facility of UAV's maneuverability and flexibility. Thus, by taking spatial retreats into account, in [27] and [28], a trajectory optimization algorithm was investigated to combat jamming signals where the UAV would fly away from the jammers while executing communication tasks. In [29], the UAV's trajectory and communication resources were jointly designed to guarantee the coexistence with the jamming signals from the terrestrial D2D GNs. Nevertheless, these works assumed that jammers' location was perfectly known. Though a robust optimization method was studied in [30], where one UAV needed to maintain the communication quality in the presence of an adversarial jammer with uncertain location information, however, considered little about the joint optimization of trajectory and communication resources for multiple UAV.

Particularly, in the multi-UAV enabled communication, the communication resources allocation for various UAV-GN pairs need to be tackled. In [31], a joint trajectory, power allocation and user scheduling algorithm was applied to mitigate the interference of system users. In [32], the UAV to UAV communication was investigated via joint trajectory and power optimization wherein the UAVs shared the same frequency. In [33] and [34], orthogonal frequency division multiple access (OFDMA) mode and time division multiple access (TDMA) mode were applied to avoid the interference of system users, respectively. Consequently, with the possible interference caused by system users, the jamming attacks from a adversarial jammer is more challenging in the multi-UAV enabled communication and has not been fully investigated.

Moreover, wireless communication systems have gradually evolved to aim not only for high throughput, but also

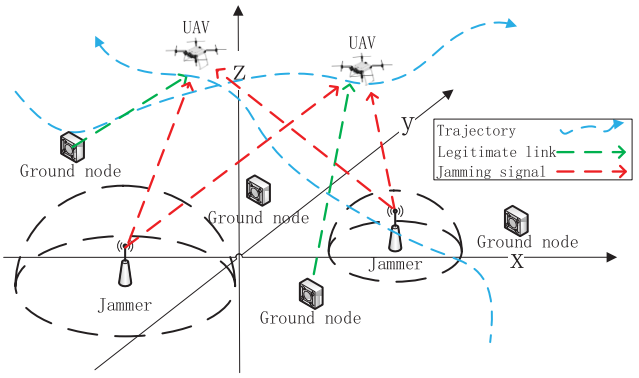

FIGURE 1. Multiple GNs are scheduled to communicate with multiple UAVs in the presence of multiple jammers with uncertain location.

for supporting highly diversified applications with heterogeneous QoS requirements. However, existing literature solely investigated a single QoS metric of the UAV-enabled communication system consists of multiple users, e.g., the minimum throughput of multiple users [4], [31] and the average throughput of multiple users [5]. Although the delay-constraint system performance metric was introduced in [33], the distinction and relation of these QoS metrics has not been analyzed so as to provide better guarantees for the diverse QoS requirements. To the best of our knowledge, the robust anti-jamming trajectory and communication design in multi-UAV enabled communication concerning different QoS requirements is still an open problem, which motivates this work. In this paper, we study a multi-UAV enabled communication system where multiple GNs are scheduled to communicate with the UAVs in the presence of multiple jammers with imperfect location information, as shown in Fig. 1. The main contribution are summarized as follows.

- We formulate a general optimization framework for the multi-UAV enabled communication in the presence of jammers with imperfect location information, which considers UAVs' trajectories, jammers' uncertain location region, the GNs' scheduling and transmit power allocation. To provide different QoS guarantees, three different optimization objectives are considered, i.e., maximizing the minimum throughput of all GNs (MMT), maximizing the average throughput of all GNs (MAT) and maximizing the minimum throughput of all GNs with delay constraint (MMTD).
- We propose a robust algorithm to solve the formulated problems which are non-convex and thus challenging to solve. Specifically, for MMT and MAT problems, we first divide the origin problem into three sub-problems that can be solved in an iterative manner by leveraging the block coordinate descend BCD) method. Then, the successive convex approximation (SCA) technique and slack variables are applied to settle the non-convexity of the sub-problems, and penalty term is introduced to handle the binary variables. Meanwhile, the infinite number of variables caused by the jammers'

imperfect location information is settled by applying the $\mathcal{S}$-Procedure. Particularly, the MMTD problem is solved via a parameter-aided BCD method since the conventional BCD method severely limits the freedom in optimization.

- Numerical results show that the proposed robust algorithms can improve the system performance significantly as compared to the benchmark algorithms for MMT, MAT and MMTD problems. Moreover, with different QoS requirements, the proposed robust algorithms can offer a considerable gain from their respective emphases, e.g., MAT can reach much higher sum throughput and minimum throughput than MMT if the worst case of GNs is acceptable in any application, giving a certain practical significance.

The remainder of the paper is organized as follows: Section II introduces the system model for the multi-UAV enabled communication system in the presence of multiple jammers. Based on this model, Section III formulates three optimization problems with different QoS consideration while Section IV, V and VI propose efficient alternating algorithms to solve them, respectively. Numerical results are provided in Section VII. Finally, Section VIII summarizes the whole work.

II. SYSTEM MODEL

We consider a multi-UAV enabled wireless network as shown in Fig. 1, where $K \geq 1$ GNs are scheduled to transmit data to $U \geq 1$ ($K \geq U$) UAVs while $M \geq 1$ jammers are sending interference signals to jam the legitimate communication. Let $\mathcal{K}$, $\mathcal{M}$ and $\mathcal{U}$ denote the the set of GNs, jammers and UAVs, respectively, where $|\mathcal{K}| = K$, $|\mathcal{M}| = M$ and $|\mathcal{U}| = U$. Without loss of generality, 3D Cartesian coordinate system is considered. Thus, the location of each GN $k \in \mathcal{K}$ and jammer $m \in \mathcal{M}$ can be denoted as $q_k = \{x_k, y_k, z_k\}$ and $q_m = \{x_m, y_m, z_m\}$, respectively. Considering the uncertain location region in 3D space, e.g., jammers mounted in skyscraper or mountain, we formulate the uncertain region of the jammers' location as a hemisphere. It is assumed that only the estimated location of jammers can be obtained, i.e., centre of the hemisphere, which is denoted as $q_{m_E} = \{x_{m_E}, y_{m_E}, z_{m_E}\}$. Hence, we have

$$x_m = x_{m_E} + \Delta x_m,\ y_m = y_{m_E} + \Delta y_m,\ z_m = z_{m_E} + \Delta z_m, \quad (1)$$

where $(\Delta x_m, \Delta y_m, \Delta z_m) \in \varepsilon_m$ is a continuous set of possible estimated errors, which satisfies the condition

$$\varepsilon_m \triangleq \left\{ \Delta x_m^2 + \Delta y_m^2 + \Delta z_m^2 \leq Q_m^2,\ \Delta z_m \geq 0 \right\}, \quad (2)$$

where Q_m is the radius of the hemisphere corresponding to jammer m.

Each UAV $u \in \mathcal{U}$ is dispatched to fly from a given start point q_u^{start} to an end point q_u^{end} over a finite time period T. However, the infinite number of variable T caused by its continues nature will make the optimization problem hard to be formulated. Thus, we divide T into N equal time slots dt so that $T = N * dt$. If dt is sufficient small, the trajectory of each UAV can be approximately denoted by the combination of discrete locations at each time slot, i.e., $\boldsymbol{Q} \triangleq \{q_u[n] = \{x_u[n], y_u[n], z_u[n]\}, \forall u, n\}$.

Considering the limited mobility of UAV, we have the following constraints as

$$q_u[0] = q_u^{start}, \quad (3)$$

$$q_u[N] = q_u^{end}, \quad (4)$$

$$\|q_u[n] - q_u[n-1]\| \leq V_{\max} dt, \quad (5)$$

$$H_{\min} \leq z_u[n] \leq H_{\max}, \forall n, \quad (6)$$

where $V_{\max}$ denotes the UAV's maximum flying speed, and $H_{\min}$ and $H_{\max}$ denote the minimum and maximum flying altitude respectively.

Frequency reuse technique is applied that the total spectrum is divided into U orthogonal channels [35]. At each time slot, one GN can associate with at most one UAV, and one UAV can associate with at most one GN. This is practically corresponding to the applications that the GNs are regarded either as ground controllers for the UAV surveillance mission or ground sensors in the UAV-supported data collection mission. Let $\boldsymbol{S} \triangleq \{s_{k,u}[n], \forall k, u, n\}$ be a binary variable that denotes the scheduling of the communication process. $s_{k,u}[n] = 1$ indicates that the GN k communicates with the UAV u at time slot n, and $s_{k,u}[n] = 0$, otherwise. Then, we have the scheduling constraints as

$$s_{k,u}[n] \in \{0, 1\}, \quad \forall u, k, n, \quad (7)$$

$$\sum_{u \in \mathcal{U}} s_{k,u}[n] \leq 1, \quad \forall k, n, \quad (8)$$

$$\sum_{k \in \mathcal{K}} s_{k,u}[n] \leq 1, \quad \forall u, n. \quad (9)$$

Considering the limited energy capacity of the GNs, let $\boldsymbol{P} \triangleq \{P_k[n], \forall k, n\}$ be the transmit power of GN k at time slot n. Then, we have the GNs' power constraints as

$$\frac{1}{N} \sum_{n \in \mathcal{N}} P_k[n] \leq P_{mean}, \quad \forall k, \quad (10)$$

$$P_k[n] \leq P_{peak}, \quad \forall k, n, \quad (11)$$

where P_{mean} and P_{peak} denote the average transmit power and the peak transmit power, respectively.

Due to the rare blockages in the air, the communication from the GNs and the jammers to the UAVs are both assumed to be LoS channels for simplicity. Hence, the channel power gain from the GN k to the UAV u at time slot n can be denoted as

$$g_{k,u}[n] = \beta_0 \|q_u[n] - q_k\|^{-\alpha}, \quad \forall k, n, \quad (12)$$

where β_0 is the channel power gain at the reference distance 1 meter, and α is the path loss exponent. Similarly, the channel power gain from the jammer m to the UAV u at time slot n can be denoted as

$$g_{m,u}[n] = \beta_0 \|q_u[n] - q_m\|^{-\alpha}, \quad \forall m, n, \quad (13)$$

Thus, the achievable throughput from the GN k to the UAV u at time slot n is given by

$$R_{k,u}[n] = \log_2\left(1 + \frac{P_k[n]g_{k,u}[n]}{\sum_{m\in\mathcal{M}} P_m g_{m,u}[n] + \sigma^2}\right), \quad \forall u, k, n, \tag{14}$$

where P_m denotes the transmit power of the jammer m, and σ^2 denotes the power of additive white Gaussian noise (AWGN) at each UAV.

III. PROBLEM FORMULATION

Considering the various QoS requirements in diverse missions, we aim to maximize three different performance metrics, i.e., MMT, MAT and MMTD, by jointly optimizing the GNs' scheduling $\boldsymbol{S}$, the GNs' transmit power $\boldsymbol{P}$ and the UAVs' trajectory $\boldsymbol{Q}$.

A. MAXIMIZING THE MINIMUM THROUGHPUT OF ALL GNS

Malicious jamming attacks may lead to serious performance decline of some specifical GNs. For example, a GN relating vital information has to be kept away form the flight area due to the terrain restrictions or the threat of armed attack. The long distance between these GNs and the UAV may lead to severe decline of performance. Thus, maximizing the minimum throughput of all GNs so as to ameliorate the GN with worst performance is of the most priority in such fairness sensitive applications. Then, we formulate the MMT problem as follows.

Based on (14), the throughput of each GN over the flight time period T can be denoted as

$$R_k = \sum_{n\in\mathcal{N}}\sum_{u\in\mathcal{U}} s_{k,u}[n]\log_2\left(1+\frac{P_k[n]g_{k,u}[n]}{\sum_{m\in\mathcal{M}} P_m g_{m,u}[n]+\sigma^2}\right), \quad \forall k, \tag{15}$$

Then, we have the optimization problem formulated as

$$\max_{\boldsymbol{S},\boldsymbol{P},\boldsymbol{Q}} \min_{k\in\mathcal{K}} R_k \tag{16a}$$
$$\text{s.t. } q_u[0] = q_u^{start}, \tag{16b}$$
$$q_u[N] = q_u^{end}, \tag{16c}$$
$$\|q_u[n] - q_u[n-1]\| \le V_{\max} dt, \tag{16d}$$
$$H_{\min} \le z_u[n] \le H_{\max}, \forall n, \tag{16e}$$
$$s_{k,u}[n] \in \{0, 1\}, \forall u, k, n, \tag{16f}$$
$$\sum_{u\in\mathcal{U}} s_{k,u}[n] \le 1, \forall k, n \tag{16g}$$
$$\sum_{k\in\mathcal{K}} s_{k,u}[n] \le 1, \forall u, n, \tag{16h}$$
$$\frac{1}{N}\sum_{n\in\mathcal{N}} P_k[n] \le P_{mean}, \forall k, \tag{16i}$$
$$P_k[n] \le P_{peak}, \forall k, n. \tag{16j}$$

B. MAXIMIZING THE AVERAGE THROUGHPUT OF ALL GNS

However, fairness is not always essential to be emphasized to ameliorate the GN with worst performance. In some cases, maximizing the average throughput of all GNs is usually the main focus. For example, in the scenario where abundant GNs relating to the same task work together to collect the information, to maximize the average throughput of all GNs is of the most importance.

Then, we have the average throughput of all GNs over the flight time period T as

$$R_a = \frac{1}{K}\sum_{n\in\mathcal{N}}\sum_{k\in\mathcal{K}}\sum_{u\in\mathcal{U}} s_{k,u}[n]\log_2\left(1+\frac{P_k[n]g_{k,u}[n]}{\sum_{m\in\mathcal{M}} P_m g_{m,u}[n]+\sigma^2}\right), \tag{17}$$

and the optimization problem is formulated as

$$\max_{\boldsymbol{S},\boldsymbol{P},\boldsymbol{Q}} R_a$$
$$\text{s.t.} \quad (16b) - (16j). \tag{18}$$

C. MAXIMIZING THE MINIMUM THROUGHPUT OF ALL GNS WITH THE DELAY CONSTRAINT

In the multi-UAV enabled wireless networks, the number of UAVs is usually much less than that of GNs. Thus, even some GNs can access to certain UAV at some time slot, they can hardly associate with UAVs all the time. However, in some delay constrained applications, transmission from the crucial GNs with higher delay priority need to be guaranteed first, i.e., such GNs need to associate with UAVs all the time rather than transmit the information within a short time. For example, a centre controller with networks' continuously updated global information need to communicate with UAVs during the whole mission.

Hence, we introduce a parameter θ_k, $\theta_k \in [0, 1]$ to denote the delay demand of user k [33]. Specifically, at each time slot n, θ_k fraction of GN's average throughput over N slots is delay-constrained and the remaining $1-\theta_k$ fraction is delay-tolerant. Then, the delay constraint of user k at time slot n can be expressed as

$$r_k[n] \ge \frac{1}{N}\theta_k R_k, \quad \forall k, n, \tag{19}$$

where

$$r_k[n] = \sum_{u\in\mathcal{U}} s_{k,u}[n]\log_2\left(1+\frac{P_k[n]g_{k,u}[n]}{\sum_{m\in\mathcal{M}} P_m g_{m,u}[n]+\sigma^2}\right), \quad \forall k, n, \tag{20}$$

which means that at any time slot n, at least θ_k fraction of the average throughput needs to be satisfied for GN k. We aim

to maximize the minimum throughput of GNs while satisfying the delay constraint. As such, we have the optimization problem formulated as

$$\max_{\boldsymbol{S},\boldsymbol{P},\boldsymbol{Q}} \min_{k\in\mathcal{K}} R_k$$
$$\text{s.t.} \quad (16b)-(16j), (19). \tag{21}$$

IV. PROPOSED ALGORITHM FOR MMT

Due to the non-smooth objective function (16a), coupled optimization variables $\boldsymbol{S}$, $\boldsymbol{P}$ and $\boldsymbol{Q}$, the binary constraints (16f), (16g) and (16h), the non-convexity of (15) along with the infinite number of estimated errors of jammers' location ε_m, problem (16) is difficult to be optimally solved. Thus, to handle the non-smooth objective function, a slack variable η is introduced and problem (16) can be reformulated without losing optimality as

$$\max_{\boldsymbol{S},\boldsymbol{P},\boldsymbol{Q},\eta} \quad \eta \tag{22a}$$
$$\text{s.t.} \quad R_k \geq \eta, \quad \forall k, \tag{22b}$$
$$(16b)-(16j).$$

However, problem (22) is still difficult to solve. To decouple the optimization variables, the BCD method can be adopted and thus the original problem can be divided into three sub-problems that can be efficiently solved. This motivates us to propose an alternating optimization based algorithm to solve (22) sub-optimally, by iteratively optimizing one of $\boldsymbol{S}$, $\boldsymbol{P}$ and $\boldsymbol{Q}$ with the other two being fixed at each iteration until convergence is reached. Then, we focus on dealing with the three sub-problems.

A. SUB-PROBLEM 1: OPTIMIZING TRANSMIT POWER WITH GIVEN TRAJECTORY AND SCHEDULING

For given trajectory $\boldsymbol{Q}$ and GNs' scheduling $\boldsymbol{S}$, to handle the unknown estimated errors ε_m, we consider the worst case that jammers are always in the closest position to the UAVs within the uncertain region. Then, problem (22) can be expressed as

$$\max_{\boldsymbol{P},\eta} \quad \eta \tag{23a}$$
$$\text{s.t.} \sum_{n\in\mathcal{N}}\sum_{u\in\mathcal{U}} s_{k,u,n}\log_2\left(1+\frac{P_k[n]g_{k,u,n}}{I_{u,n}}\right)\geq\eta, \quad \forall k,$$
$$(16i), (16j), \tag{23b}$$

where

$$I_{u,n} = \sum_{m\in\mathcal{M}} P_m g_{m,u,n} + \sigma^2, \tag{24}$$
$$g_{m,u,n} = \beta_0\left(\left\|q_u[n]-q_{m_E}\right\|-Q_m\right)^{-\alpha}. \tag{25}$$

It is a standard convex optimization problem, which can be efficiently solved by some existing algorithms such as the interior point method with CVX [36].

B. SUB-PROBLEM 2: OPTIMIZING SCHEDULING WITH GIVEN TRANSMIT POWER AND TRAJECTORY

To tackle the binary variables $\boldsymbol{S}$, we relax it into continuous variables $\tilde{\boldsymbol{S}} \triangleq \left\{0\leq\tilde{s}_{k,u}[n]\leq 1, \forall k,u,n\right\}$. Thus, for given transmit power $\boldsymbol{P}$ and trajectory $\boldsymbol{Q}$, problem (22) can be transformed as

$$\max_{\tilde{\boldsymbol{S}},\eta} \quad \eta \tag{26a}$$
$$\text{s.t.} \sum_{n\in\mathcal{N}}\sum_{u\in\mathcal{U}} \tilde{s}_{k,u}[n]\log_2\left(1+\frac{P_{k,u,n}g_{k,u,n}}{I_{u,n}}\right)\geq\eta, \quad \forall k, \tag{26b}$$
$$0\leq\tilde{s}_{k,u}[n]\leq 1, \quad \forall k,u,n, \tag{26c}$$
$$(16g), (16h).$$

Through such relaxation, the objective value of problem (26) provides an upper bound for that of the origin sub-problem. However, this method usually leads to undesired user scheduling and association when $\tilde{s}_{k,u}[n]$ doesn't have evident tendency towards 0 or 1. We note that $\tilde{s}_{k,u}[n]^2\geq\tilde{s}_{k,u}[n]$, $0\leq\tilde{s}_{k,u}[n]\leq 1, \forall u,k,n,$ is equivalent to (16f). Then, inspired by this binary nature, a penalty term is introduced to the objective function (26a). Hence, problem (26) can be reformulated as

$$\max_{\tilde{\boldsymbol{S}},\eta} \quad \eta+\lambda\sum_{n\in\mathcal{N}}\sum_{k\in\mathcal{K}}\sum_{u\in\mathcal{U}}\left(\tilde{s}_{k,u}^2[n]-\tilde{s}_{k,u}[n]\right)$$
$$\text{s.t.} \quad (16g), (16h), (26b), (26c), \tag{27}$$

where λ is a nonnegative constant to ensure $\tilde{s}_{k,u}[n]$ approaches to 0 or 1.

Nevertheless, the term $\tilde{s}_{u,k}^2[n]$ makes the objective function in problem (27) a convex function, and a maximization problem with a convex objective function is intractable to be optimally solved. Thus, with the property that the convex function's first-order Taylor expansion provides a global under-estimator at the feasible point, we have

$$\tilde{s}_{k,u}^2[n]\geq 2\tilde{s}_{k,u}^f[n]\tilde{s}_{k,u}[n]-\left(\tilde{s}_{k,u}^f[n]\right)^2, \tag{28}$$

where $\tilde{s}_{k,u}^f[n]$ is the feasible point of $\tilde{s}_{k,u}[n]$. Then, we derive a lower bound of problem (27) as

$$\max_{\tilde{\boldsymbol{S}},\eta} \quad \eta+\lambda\sum_{n\in\mathcal{N}}\sum_{k\in\mathcal{K}}\sum_{u\in\mathcal{U}}\left(2\tilde{s}_{k,u}^f[n]\tilde{s}_{k,u}[n]-\left(\tilde{s}_{k,u}^f[n]\right)^2-\tilde{s}_{k,u}[n]\right)$$
$$\text{s.t.} \quad (16g), (16h), (26b), (26c). \tag{29}$$

Problem (29) is a standard linear programming (LP) problem, which can be solved via CVX [36].

C. SUB-PROBLEM 3: OPTIMIZING TRAJECTORY WITH GIVEN SCHEDULING AND TRANSMIT POWER

For given GNs' scheduling $\boldsymbol{S}$ and transmit power $\boldsymbol{P}$, problem (22) can be expressed as

$$\max_{\boldsymbol{Q},\eta} \quad \eta \tag{30a}$$

$$\text{s.t.} \sum_{n\in\mathcal{N}}\sum_{u\in\mathcal{U}} s_{k,u,n}\log_2\left(1+\frac{P_{k,n}g_{k,u}[n]}{\sum\limits_{m\in\mathcal{M}} P_m g_{m,u}[n]+\sigma^2}\right)\geq\eta, \quad \forall k,$$
$$(16b), (16c), (16d), (16e). \tag{30b}$$

Problem (30) is non-convex due to the term $g_{k,u}[n] = \beta_0\|q_u[n]-q_k\|^{-\alpha}$, $\forall k, u$ and $g_{m,u}[n] = \beta_0\|q_u[n]-q_m\|^{-\alpha}$, $\forall m, u$. Thus, by introducing two slack variables $\boldsymbol{L} = \{L_{k,u}[n], \forall k, u, n\}$ and $\boldsymbol{I} = \{I_u[n], \forall u, n\}$, problem (30) can be rewritten as

$$\max_{\boldsymbol{Q},\boldsymbol{L},\boldsymbol{I},\eta} \ \eta \tag{31a}$$
$$\text{s.t.} \sum_{n\in\mathcal{N}}\sum_{u\in\mathcal{U}} s_{k,u,n}\log_2\left(1+\frac{1}{L_{k,u}[n]I_u[n]}\right)\geq\eta, \quad \forall k, \tag{31b}$$
$$P_{k,n}g_{k,u}[n]\geq L_{k,u}[n]^{-1}, \quad \forall k, u, n, \tag{31c}$$
$$\sum_{m\in\mathcal{M}} P_m g_{m,u}[n]+\sigma^2\leq I_u[n], \quad \forall u, n, \tag{31d}$$
$$(16b), (16c), (16d), (16e).$$

The equivalence of (30) and (31) can be proved by contradiction. Particularly, when $P_{k,n}\beta_0\|q_u[n]-q_k\|^{-\alpha} = L_{k,u}[n]^{-1}$, $\forall k, u, n$ and $\sum\limits_{m\in\mathcal{M}} P_m\beta_0\|q_u[n]-q_m\|^{-\alpha}+\sigma^2 = I_u[n]$, $\forall u, n$ hold, problem (30) and (31) share the same optimal solution. If the constraints (31c) and (31d) hold with inequalities when the optimal solution of (31) is obtained, we can always decrease $L_{k,u}[n]$ and $I_u[n]$ to improve the objective value. Thus, problem (30) and (31) can achieve the same optimal solution.

In the next step, we focus on dealing with problem (31). Note that constraint (31b) and (31d) are still non-convex, we resort to the following lemma by applying SCA.

Lemma 1: Constraint (31b) is lower bounded at the feasible point $(L^f_{k,u}[n], I^f_u[n])$ by

$$\begin{aligned}&R_{lb}\left(L_{k,u}[n], I_u[n]\right)\\&= s_{k,u,n}\log_2(1+1/L^f_{k,u}[n]I^f_u[n])\\&\quad+s_{k,u,n}A_{k,u}(L_{k,u}[n]-L^f_{k,u}[n])+s_{k,u,n}B_{k,u}(I_u[n]-I^f_u[n]),\end{aligned} \tag{32}$$

where $A_{k,u} = -\log_2 e/(L^f_{k,u}[n]+(L^f_{k,u}[n])^2 I^f_u[n])$ and $B_{k,u} = -\log_2 e/(I^f_u[n]+(I^f_u[n])^2 L^f_{k,u}[n])$.

Proof: Since $f(x,y) = \log_2(1+1/xy)$ is a convex function, its first-order Taylor expansion provides a global under-estimator at a feasible point (x^f, y^f), i.e.,

$$\begin{aligned}\log_2(1+1/xy)\geq\ &\log_2(1+1/x^f y^f)\\&-(x-x^f)\log_2 e/(x^f+(x^f)^2y^f)\\&-(y-y^f)\log_2 e/(y^f+(y^f)^2x^f).\end{aligned} \tag{33}$$

Thus, by applying $x = L_{k,u}[n]$, $y = I_u[n]$, Lemma 1 is proved. ∎

Then, we introduce slack variable $\boldsymbol{D} = \{d_{m,u}[n], \forall m, u, n\}$ to deal with the non-convexity of constraint (31d) that

$$d_{m,u}[n]\leq\|q_u[n]-q_m\|^2, \quad \forall m, u, n, \tag{34}$$

and

$$d_{m,u}[n]\geq 0, \quad \forall m, u, n. \tag{35}$$

Then, the constraint (31d) can be transformed into a convex form as

$$\sum_{m\in\mathcal{M}} P_m\beta_0 d_{m,u}[n]^{-\alpha/2}+\sigma^2\leq I_u[n], \quad \forall m, u. \tag{36}$$

Hence, (31) can be equivalently written as

$$\max_{\boldsymbol{Q},\boldsymbol{L},\boldsymbol{I},\boldsymbol{D},\eta} \ \eta \tag{37a}$$
$$\text{s.t.} \sum_{n\in\mathcal{N}}\sum_{u\in\mathcal{U}} R_{lb}\left(L_{k,u}[n], I_u[n]\right)\geq\eta, \quad \forall k, \tag{37b}$$
$$d_{m,u}[n]\leq\|q_u[n]-q_m\|^2, \forall m, u, n, \tag{37c}$$
$$d_{m,u}[n]\geq 0, \quad \forall m, u, n, \tag{37d}$$
$$(16b), (16c), (16d), (16e), (31c), (36).$$

Problem (37) and (31) have the same optimal solution for the constraint (37c) should hold with equality when the optimal solution of both problem are obtained. Otherwise, $d_{m,u}[n]$ can be increased to enhance the value of objective function of problem (37) until the equality of the constraint (37c) is obtained.

Note the term q_m in (37c) contains infinite number of variables due to the constraints of jammers' uncertain location (1) and (2). Then, with (1) and (2), (37c) is reformulated as

$$\Delta x_m^2+\Delta y_m^2+\Delta z_m^2-Q_m^2\leq 0, \forall m, \tag{38}$$

and

$$\begin{aligned}&-\left(x_{m_E}+\Delta x_m-x_u[n]\right)^2-\left(y_{m_E}+\Delta y_m-y_u[n]\right)^2\\&-\left(z_{m_E}+\Delta z_m-z_u[n]\right)^2+d_{m,u}[n]\leq 0, \quad \forall m, u, n,\end{aligned} \tag{39}$$

Then, according to $\mathcal{S}$-Procedure [37], since there exists a point $\left(\Delta\hat{x}_m, \Delta\hat{y}_m, \Delta\hat{z}_m\right)$, e.g., $\left(\Delta\hat{x}_m, \Delta\hat{y}_m, \Delta\hat{z}_m\right) = (0,0,0)$, making $\Delta x_m^2+\Delta y_m^2+\Delta z_m^2-Q_m^2\leq 0$, the implication (38)→(39) holds only if there exists $\boldsymbol{\xi}\triangleq\{\xi_m[n]\geq 0, \forall m, n\}$ such that

$$\Phi\left(x_u[n], y_u[n], z_u[n], d_{m,u}[n], \xi_m[n]\right)\succeq 0, \quad \forall m, u, n, \tag{40}$$

where

$$\begin{aligned}&\Phi\left(x_u[n], y_u[n], z_u[n], d_{m,u}[n], \xi_m[n]\right)\\&=\begin{bmatrix}\xi_m[n]+1 & 0 & 0 & x_{m_E}-x_u[n]\\ 0 & \xi_m[n]+1 & 0 & y_{m_E}-y_u[n]\\ 0 & 0 & \xi_m[n]+1 & z_{m_E}-z_u[n]\\ X[n] & Y[n] & Z[n] & Q_c[n]\end{bmatrix}\end{aligned} \tag{41}$$

and $X[n] = x_{m_E}-x_u[n]$, $Y[n] = y_{m_E}-y_u[n]$, $Z[n] = z_{m_E}-z_u[n]$, $Q_c[n] = -Q_m^2\xi_m[n]+c_{m,u}[n]$, and

$$\begin{aligned}&c_{m,u}[n]\\&= x_u^2[n]-2x_{m_E}x_u[n]+x_{m_E}^2+y_u^2[n]-2y_{m_E}y_u[n]\\&\quad+y_{m_E}^2+z_u^2[n]-2z_{m_E}z_u[n]+z_{m_E}^2-d_{m,u}[n], \quad \forall m, u, n,\end{aligned} \tag{42}$$

Further, with the first-order Taylor expansion of the convex function, the lower bound of the term $x_u^2[n]$, $y_u^2[n]$ and $z_u^2[n]$ in (42) can be obtained and (42) can be transformed as

$$\begin{aligned}\tilde{c}_{m,u}[n] = &-\left(x_u^f[n]\right)^2 + 2x_u^f[n]x_u[n] - 2x_{m_E}x_u[n] \\ &+ x_{m_E}^2 - \left(y_u^f[n]\right)^2 + 2y_u^f[n]y_u[n] - 2y_{m_E}y_u[n] \\ &+ y_{m_E}^2 - \left(z_u^f[n]\right)^2 + 2z_u^f[n]z_u[n] - 2z_{m_E}z_u[n] \\ &+ z_{m_E}^2 - d_{m,u}[n], \quad \forall m, u, n \end{aligned} \tag{43}$$

Finally, by substituting $\tilde{c}_{m,u}[n]$ into $Q_c[n]$ in (41) as $\tilde{Q}_c[n] = -Q_m^2\xi_m[n] + \tilde{c}_{m,u}[n]$, problem (37) is rewritten as

$$\max_{\boldsymbol{Q},\boldsymbol{L},\boldsymbol{I},\boldsymbol{D},\boldsymbol{\xi},\eta} \quad \eta \tag{44a}$$

$$\text{s.t. } \tilde{\Phi}\left(x_u[n], y_u[n], z_u[n], d_{m,u}[n], \xi_m[n]\right) \succeq 0, \forall m, u, n, \tag{44b}$$

$$\xi_m[n] \geq 0, \quad \forall m, \tag{44c}$$

$$(16b), (16c), (16d), (16e), (31c), (36), (37b), (37d).$$

where

$$\tilde{\Phi}\left(x_u[n], y_u[n], z_u[n], d_{m,u}[n], \xi_m[n]\right) = \begin{bmatrix} \xi_m[n]+1 & 0 & 0 & x_{m_E} - x_u[n] \\ 0 & \xi_m[n]+1 & 0 & y_{m_E} - y_u[n] \\ 0 & 0 & \xi_m[n]+1 & z_{m_E} - z_u[n] \\ X[n] & Y[n] & Z[n] & \tilde{Q}_c[n] \end{bmatrix} \tag{45}$$

Problem (44) is a semidefinite programming problem and can be optimally solved by CVX [36].

D. OVERALL ALGORITHM

In conclusion, the proposed algorithm divides the original problem (16) into three sub-problems by applying the BCD method. Specifically, **sub-problem** 1 is a convex optimization problem as (23). With the assist of penalty term and SCA technique, **sub-problem** 2 is solved in a standard LP form as (29). With the introduction of slack variables, SCA technique and $\mathcal{S}$-Procedure, **sub-problem** 3 is solved as a semidefinite programming problem as (44). We solve them in an iterative way until the fractional increase of the objective function is below a small threshold μ. The obtained solution of each sub-problem is nondecreasing over iterations while the value of the original problem is finite. Thus, the proposed algorithm is guaranteed to converge. The details of the proposed algorithm are presented in **Algorithm 1**.

V. PROPOSED ALGORITHM FOR MAT

Note that the optimization problems MAT and MMT share the same optimization constraints (16b)-(16j) and differ in the objective function, i.e., (18) and (16a). Thus, we can directly formulate the three sub-problems and solve them in a iterative manner.

Algorithm 1 The Proposed Algorithm for Solving Problem (16)

1: **Initialization:** set $i = 0$, an initial feasible solution $\left(\boldsymbol{S}^{(i)}, \boldsymbol{P}^{(i)}, \boldsymbol{Q}^{(i)}\right)$.
2: **Repeat**
3: With given $\boldsymbol{S}^{(i)}$ and $\boldsymbol{Q}^{(i)}$, update $\boldsymbol{P}^{(i)}$ to $\boldsymbol{P}^{(i+1)}$ by solving sub-problem 1
4: With given $\boldsymbol{P}^{(i+1)}$ and $\boldsymbol{Q}^{(i)}$, update $\boldsymbol{S}^{(i)}$ to $\boldsymbol{S}^{(i+1)}$ with obtained $\tilde{\boldsymbol{S}}$ by solving sub-problem 2
5: With given $\boldsymbol{S}^{(i+1)}$ and $\boldsymbol{P}^{(i+1)}$, update $\boldsymbol{Q}^{(i)}$ to $\boldsymbol{Q}^{(i+1)}$ by solving sub-problem 3
6: Update $i \leftarrow i + 1$
7: **Until** The fractional increase of the objective value is below a small threshold μ.

A. SUB-PROBLEM 1: OPTIMIZING TRANSMIT POWER WITH GIVEN TRAJECTORY AND SCHEDULING

Based on (24) and (25), we have

$$\begin{aligned}&\max_{\boldsymbol{P}} \frac{1}{K}\sum_{n\in\mathcal{N}}\sum_{k\in\mathcal{K}}\sum_{u\in\mathcal{U}} s_{k,u,n}\log_2\left(1 + \frac{P_k[n]g_{k,u,n}}{I_{u,n}}\right) \\ &\text{s.t. } (16i), (16j). \end{aligned} \tag{46}$$

which is a convex optimization problem that can be efficiently solved by CVX [36].

B. SUB-PROBLEM 2: OPTIMIZING SCHEDULING WITH GIVEN TRANSMIT POWER AND TRAJECTORY

With $\tilde{\boldsymbol{S}} \triangleq \left\{0 \leq \tilde{s}_{k,u}[n] \leq 1, \forall k, u, n\right\}$, penalty term is also introduced to the objective function. Then, we formulate the optimization problem as

$$\begin{aligned}&\max_{\tilde{\boldsymbol{S}}} \frac{1}{K}\sum_{n\in\mathcal{N}}\sum_{k\in\mathcal{K}}\sum_{u\in\mathcal{U}} \tilde{s}_{u,k}[n]\log_2\left(1 + \frac{P_{u,k,n}g_{u,k,n}}{I_{u,n}}\right) \\ &\quad + \lambda\sum_{n\in\mathcal{N}}\sum_{k\in\mathcal{K}}\sum_{u\in\mathcal{U}}\left(2\tilde{s}_{k,u}^f[n]\tilde{s}_{k,u}[n] - \left(\tilde{s}_{k,u}^f[n]\right)^2 - \tilde{s}_{k,u}[n]\right) \\ &\text{s.t. } (16g), (16h), (26b), (26c). \end{aligned} \tag{47}$$

which is a standard linear programming (LP) problem that can be solved via CVX [36].

C. SUB-PROBLEM 3: OPTIMIZING TRAJECTORY WITH GIVEN SCHEDULING AND TRANSMIT POWER

With the lower bound derived in Lemma 1 and $\mathcal{S}$-Procedure, we have the optimization problem as

$$\begin{aligned}&\max_{\boldsymbol{Q}} \frac{1}{K}\sum_{n\in\mathcal{N}}\sum_{k\in\mathcal{N}}\sum_{u\in\mathcal{U}} R_{lb}\left(L_{k,u}[n], I_u[n]\right) \\ &\text{s.t. } (16b), (16c), (16d), (16e), (31c), (36), (37d), (44b), (44c). \end{aligned} \tag{48}$$

which is also a semidefinite programming problem that can be optimally solved by CVX [36].

D. OVERALL ALGORITHM

The proposed algorithm for MAT also divides the original problem into three sub-problems by applying the BCD method. The obtained solution of each sub-problem is nondecreasing over iterations while the value of the original problem is finite. Thus, the solution is guaranteed to converge. Hence, the MAT problem can be solved with **Algorithm 1** as well.

VI. PROPOSED ALGORITHM FOR MMTD

Note that the optimization problems MMTD and MMT only differ in the constraint (19), which is non-convex thus makes the MMTD problem more intractable. Thus, similar to problem (22), we first formulate the MMTD problem without losing optimality as

$$\max_{\boldsymbol{S},\boldsymbol{P},\boldsymbol{Q},\eta} \ \eta \quad \text{s.t. } (16b)-(16j),\ (19),\ (22b). \tag{49}$$

Note that $r_k[n]$ and R_k jointly make (19) non-convex. Hence, to facilitate the development of trackable sub-problems, we convert problem (49) as follows,

$$\max_{\boldsymbol{S},\boldsymbol{P},\boldsymbol{Q},\eta} \ \eta \tag{50a}$$

$$\text{s.t. } r_k[n] \geq \frac{1}{N}\theta_k\eta, \quad \forall k,n, \tag{50b}$$

$$(16b)-(16j),\ (22b).$$

Comparing problem (50) with (49), the feasible solution of problem (49) is a subset of that of problem (50). However, they can obtain the same optimal solution when the GNs achieve the equal average throughput. This can be verified by contradiction since otherwise, the optimal value of (49) can be further improved by allocating more resources to the GN with a lower throughput within the total transmit power and scheduling constraints.

Note problems (50) and (22) only differ in (50b). Thus, by adding constraint (50b) into the three sub-problems formulated from problem (22), we formulate the three trackable sub-problems of MMTD.

A. SUB-PROBLEM 1: OPTIMIZING TRANSMIT POWER WITH GIVEN TRAJECTORY AND SCHEDULING

For given trajectory $\boldsymbol{Q}$ and GNs' scheduling $\boldsymbol{S}$, (50b) can be written as (51b), and the optimization problem can be formulated as

$$\max_{\boldsymbol{P},\eta} \ \eta \tag{51a}$$

$$\text{s.t.} \sum_{u\in\mathcal{U}} s_{k,u,n}\log_2\left(1+\frac{P_k[n]g_{k,u,n}}{\sum_{m\in\mathcal{M}} P_m g_{m,u,n}+\sigma^2}\right)\geq\frac{1}{N}\theta_k\eta, \quad \forall k,n,$$

$$(16i),\ (16j),\ (23b). \tag{51b}$$

which is a convex optimization problem that can be efficiently solved by CVX [36].

B. SUB-PROBLEM 2: OPTIMIZING SCHEDULING WITH GIVEN TRANSMIT POWER AND TRAJECTORY

With $\tilde{\boldsymbol{S}} \triangleq \left\{0\leq\tilde{s}_{k,u}[n]\leq 1,\forall k,u,n\right\}$, (50b) can be written as (52b), and the optimization problem can be formulated as

$$\max_{\tilde{\boldsymbol{S}},\lambda,\eta} \ \eta+\lambda\sum_{n\in\mathcal{N}}\sum_{k\in\mathcal{K}}\sum_{u\in\mathcal{U}}\left(2\tilde{s}^f_{k,u}[n]\tilde{s}_{k,u}[n]-\left(\tilde{s}^f_{k,u}[n]\right)^2-\tilde{s}_{k,u}[n]\right) \tag{52a}$$

$$\text{s.t.} \sum_{u\in\mathcal{U}}\tilde{s}_{k,u}[n]\log_2\left(1+\frac{P_{k,n}g_{k,u,n}}{\sum_{m\in\mathcal{M}} P_m g_{m,u,n}+\sigma^2}\right)\geq\frac{1}{N}\theta_k\eta,\ \forall k,n, \tag{52b}$$

$$(16g),\ (16h),\ (26b),\ (26c).$$

which is also a standard linear programming (LP) problem that can be solved via CVX [36].

C. SUB-PROBLEM 3: OPTIMIZING TRAJECTORY WITH GIVEN SCHEDULING AND TRANSMIT POWER

Similarly, (50b) can be written as (53b), and the optimization problem can be formulated as

$$\max_{\boldsymbol{Q},\boldsymbol{L},\boldsymbol{I},\boldsymbol{D},\boldsymbol{\xi},\eta} \ \eta \tag{53a}$$

$$\text{s.t.} \sum_{u\in\mathcal{U}} s_{k,u,n}\log_2\left(1+\frac{P_{k,n}g_{k,u}[n]}{\sum_{m\in\mathcal{M}} P_m g_{m,u}[n]+\sigma^2}\right)\geq\frac{1}{N}\theta_k\eta, \quad \forall k,n, \tag{53b}$$

$$(16b),(16c),(16d),(16e),(31c),$$
$$(36),(37b),(37d),(44b),(44c).$$

However, constraint (53b) is non-convex. Thus, with the introduced two slack variables $\boldsymbol{L}=\left\{L_{k,u}[n],\forall k,u,n\right\}$ and $\boldsymbol{I}=\{I_u[n],\forall u,n\}$, the lower bound derived in Lemma 1 and $\mathcal{S}$-Procedure, we have the optimization problem transformed as

$$\max_{\boldsymbol{Q},\boldsymbol{L},\boldsymbol{I},\boldsymbol{D},\boldsymbol{\xi},\eta} \ \eta \tag{54a}$$

$$\text{s.t. } R_{lb}\left(L_{k,u}[n],I_u[n]\right)\geq\frac{1}{N}\theta_k\eta, \quad \forall k,n, \tag{54b}$$

$$(16b),(16c),(16d),(16e),(31c),(36),(37b),$$
$$(37d),(44b),(44c).$$

which is a semidefinite programming problem that can be optimally solved by CVX [36].

D. OVERALL ALGORITHM

The three sub-problems can also be optimally solved respectively. However, employing **Algorithm 1** directly for our MMTD problem will lead to unsuccessful update of the UAVs' trajectories, which can be observed from the delay constraint (53b), i.e., for given $P_{k,n}$ and $s_{k,u,n}$, since problem (53) aims to increase η by optimizing UAVs' trajectory $q[n]$, the right hand side of (53b) is expected to increase in

each iteration. Nevertheless, for any GN k that have met constraints in (51b) or (52b) with equality in the latest iteration, the only way to improve the value of η in the current iteration is to either increase $g_{k,u}[n]$ or decrease $\sum_{m\in\mathcal{M}} P_m g_{m,u}[n]$ in (53b). This observation implies that the UAV's location $q[n]$ needs to be changed to decrease the distances from the UAV to all GNs while keeping the UAV in a proper location that enables the $P_m g_{m,u}[n]$ non-increasing. Hence, the freedom of optimization for trajectory is severely limited, which will lead to an ineffective iteration of UAV's trajectory optimization.

To tackle this issue, a parameter-aided block coordinate descent algorithm is introduced. Denote θ_k^{temp} as the temporary delay constraint ratio for GN k in any iteration and initialize it as θ_k^{ini}, which is lager than the desired θ_k. In each iteration, θ_k^{temp} is made gradually decreased with a predefined step size $\theta_k^{step} > 0$ until the desired value of θ_k is achieved, through which η can be increased after each iteration while the constraint (53b) will be relaxed due to the decrease of θ_k^{temp}. Thus, the UAVs' trajectory updates in a more effective way compared to the conventional BCD method. What's more, the proposed algorithm generates a feasible solution for the original problem (50) for the desired θ_k will be eventually reached. The details of the proposed algorithm are summarized in **Algorithm 2**. The number of iterations required for starting from the initial θ_k^{ini} to the target θ_k is denoted by I_{count}.

Algorithm 2 The Proposed Algorithm Based on Parameter-Aided Block Coordinate Descent Method for Solving Problem (50)

1: **Initialization:** set $i = 0$, $\theta_k^{temp} = \theta_k^{ini}$ and I_{count}, thus $\theta_k^{step} = \frac{\theta_k^{ini} - \theta_k}{I_{count}}$.
2: **Repeat**
3: With given $\boldsymbol{S}^{(i)}$ and $\boldsymbol{Q}^{(i)}$, update $\boldsymbol{P}^{(i)}$ to $\boldsymbol{P}^{(i+1)}$ by solving sub-problem 1
4: With given $\boldsymbol{P}^{(i+1)}$ and $\boldsymbol{Q}^{(i)}$, update $\boldsymbol{S}^{(i)}$ to $\boldsymbol{S}^{(i+1)}$ with obtained $\tilde{\boldsymbol{S}}$ by solving sub-problem 2
5: $\theta_k^{temp} = \max\{\theta_k^{temp} - (i+1)\theta_k^{step}, \theta_k\}, \forall k$
6: With given θ_k^{temp}, $\boldsymbol{S}^{(i+1)}$ and $\boldsymbol{P}^{(i+1)}$, update $\boldsymbol{Q}^{(i)}$ to $\boldsymbol{Q}^{(i+1)}$ by solving sub-problem 3
7: Update $i \leftarrow i + 1$
8: **Until** $\theta_k^{temp} = \theta_k$, and the fractional increase of the objective value is below a small threshold μ.

VII. NUMERICAL RESULTS

In this section, numerical results are provided to evaluate the performance of our proposed algorithms. Note that **Algorithm 1** and **Algorithm 2** both optimize the blocks of variables alternatively and share the same robust optimization process, we first verify **Algorithm 1** for MMT that jointly optimizes UAV's trajectory, GNs' transmit power and scheduling (Joint robust optimization) for problem (16) along with the following three benchmark algorithms, i.e., robust trajectory optimization without GNs' scheduling and transmit power optimization (Robust trajectory optimization), nonrobust trajectory optimization without GNs' scheduling and transmit power optimization (Nonrobust trajectory optimization), fixed trajectory, GNs' scheduling and transmit power for initialization (Fixed initialization). Specifically, the "Nonrobust trajectory optimization" is a special case of the "Robust trajectory optimization" while assuming $Q_m = 0$. The "Fixed initialization" allocates the transmit power and scheduling equally and the UAV's trajectory is a straight line from the start point to the end point.

The parameters are set as follows. The flight time $T = 20s$ and the time slot $dt = 0.5s$. Without loss of generality, $U = 3$ UAVs are lunched for the mission, whose start and end point are set as $(0, 0, 50)$ and $(500, 0, 150)$ for UAV 1, $(50, 100, 120)$ and $(450, -100, 70)$ for UAV 2, $(50, -100, 70)$ and $(450, 100, 120)$ for UAV 3. There are $K = 6$ GNs whose location are set as $(100, -200, 0)$, $(200, 50, 0)$, $(400, 200, 0)$, $(100, 200, 0)$, $(300, -50, 0)$, $(400, -200, 0)$, respectively. There are $M = 2$ jammers whose estimated location are $(100, -50, 0)$ with $Q_1 = 30$ and $(400, 50, 0)$ with $Q_2 = 110$, respectively. The minimum flying altitude $H_{min} = 50$ and the maximum flying altitude $H_{max} = 150$. The maximum speed of UAVs $V = 60m/s$. Unless otherwise specified, the power of jamming signal $P_m = 0.4$ W, the average transmit power $p_{mean} = 0.2$ W. The peak transmit power $P_{peak} = 0.5$ W. Each UAV-GN pair is allocated with a unit bandwidth. The noise power spectrum density is -169 dBm/Hz. The channel power gain at the reference distance $d_0 = 1$ m is $\beta_0 = -30$ dB. The path loss exponent $\alpha = 2$. The penalty term $\lambda = \frac{1}{KUN}$. The convergence threshold $\mu = 10^{-3}$.

Fig. 2 shows the trajectories of three UAVs of our proposed algorithm "Joint robust optimization". The start points have been labeled with "UAV1", "UAV2" and "UAV3". The "Fixed initialization" algorithm is used here to initialize the feasible point of the variables, i.e., UAV 1 associates with GN 2 in the first half of the whole flight time slots and associates with GN 5 in the rest time slots, and so are UAV 2 associates with GN 4 and GN 6 and UAV 3 associates with GN 1 and GN 3. All the GNs' transmit power are equally allocated as $P_k[n] = P_{mean}, \forall k, n$. Trajectories of UAVs are line segment from the start point to the end point. This is intuitively reasonable for that the start point and the end point of UAV 1 are closer to GN 2 and GN 5, respectively. The same reason is for UAV 2 and UAV 3. It can be seen that the UAVs fly in a curve to resist the jamming signals and hover in some specifical location due to the GNs' scheduling and transmit power allocation. However, such illustration for trajectories of UAVs can not reveal the impact of our proposed algorithm "Joint robust optimization" in deep. Hence, we study the impact of the robust design of our proposed algorithm by leveraging the "Robust trajectory optimization" and the "Nonrobust trajectory optimization".

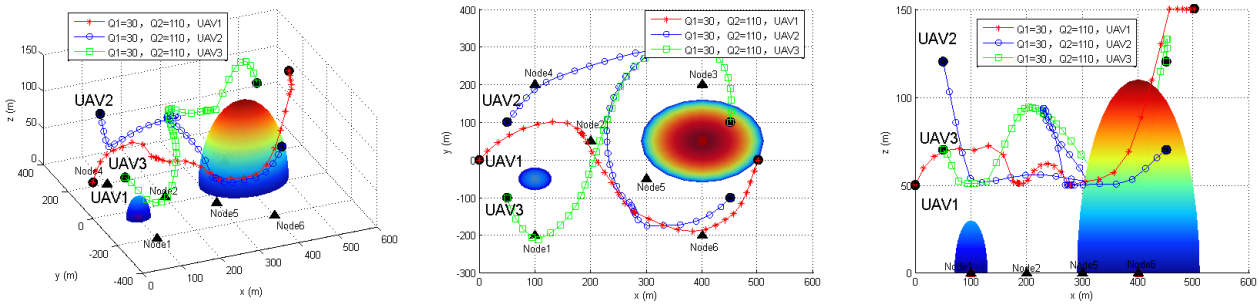

(a) View 1 (b) View 2 (c) View 3

FIGURE 2. UAVs' trajectory of our proposed "Joint robust optimization" algorithm in different view.

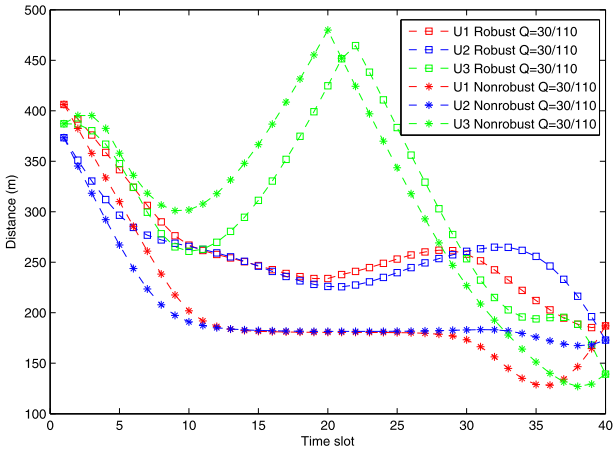

FIGURE 3. Three UAVs' distance to jammer 2 of "Robust trajectory optimization" and "Nonrobust trajectory optimization".

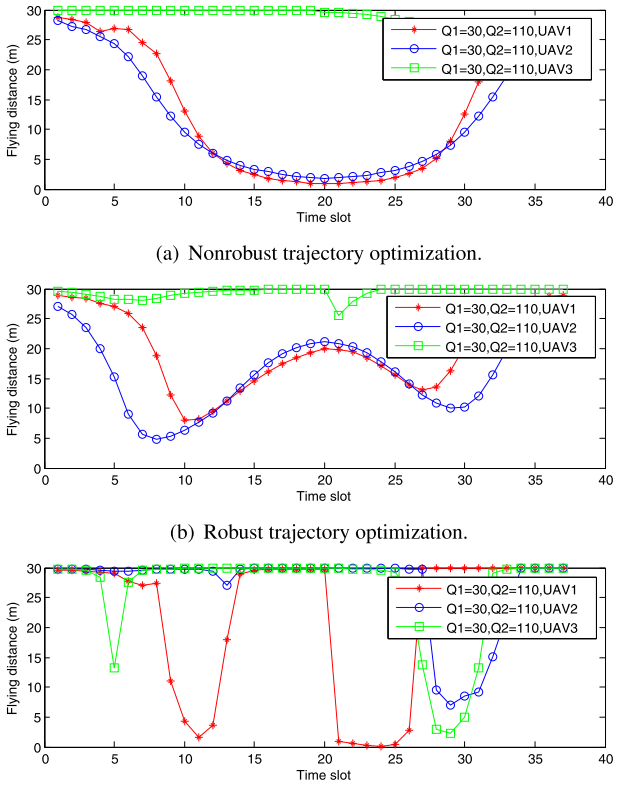

(a) Nonrobust trajectory optimization.

(b) Robust trajectory optimization.

(c) Joint robust optimization.

FIGURE 4. UAVs' flying distance at each time slot (relative speed).

As shown in Fig. 3, we compare the UAVs' distance to jammer 2 of the "Robust trajectory optimization" and the "Nonrobust trajectory optimization" during the whole flight, respectively. It can be seen that the distance to jammer 2 of UAV 1 and UAV 2 in the "Robust trajectory optimization" are always larger than that in the "Nonrobust trajectory optimization". This is because jammer 2 has a broader range of the uncertain region than jammer 1 so that the UAV have to fly farther to combat the jamming signals. Particularly, the distance to jammer 2 of UAV 3 in the "Robust trajectory optimization" is smaller than that in the "Nonrobust trajectory optimization" in the first half of the flight time for that in certain locations, UAV 3 is relatively closer to jammer 1 and farther to jammer 2. In other words, the impact of jammer 1 is greater than jammer 2 to the corresponding communication links. Thus, UAV 3 has to fly farther from jammer 1 to combat the jamming signals. Through this, the robust design in our proposed algorithm is verified.

Then, to verify the GNs' scheduling and transmit power allocation, we first illustrate the UAVs' flying distance at each time slot (relative speed) of the three algorithms. In Fig. 4(a), it can be observed that UAVs fly with the speed that with a smooth change. This is because in the "Nonrobust trajectory optimization", UAV 1 and UAV 2 are mostly hovering in a certain location with a relative low speed in the middle of the time slots so as to achieve a optimal system performance. In Fig. 4(b), UAV 2 flies close to GN 4 with a decreasing speed until reaching the optimal location associated with GN4. Then, UAV 2 speeds up to avoid the jamming signals. The same process is applicable when UAV 2 is associated with GN 6. This is because in the "Robust trajectory optimization", due to the aggravated jamming threat caused by jammers' uncertain regions, UAVs have to communicate with the corresponding GNs in their respective optimal location. In Fig.4(c), the relative speed of UAVs changed sharply in certain location. This is because in the "Joint robust optimization", the trajectory can further be optimized to achieve a better system performance owing to the adjustable

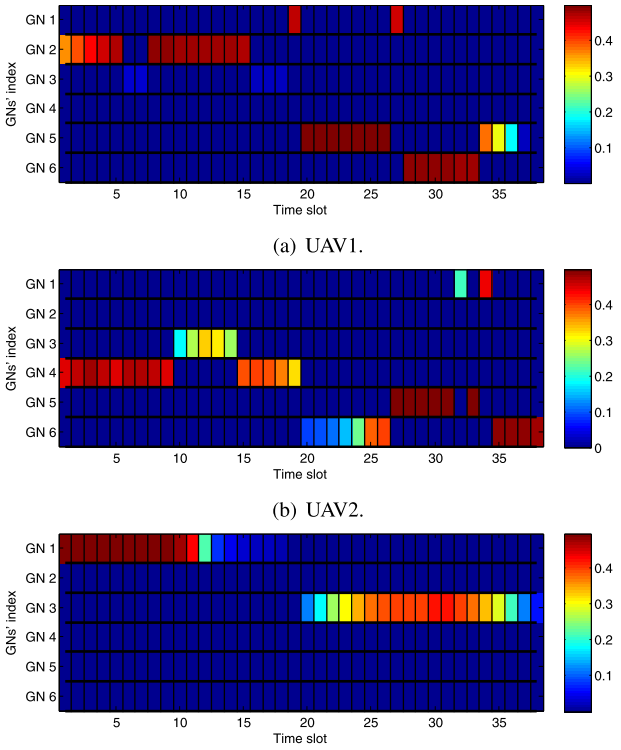

(a) UAV1.

(b) UAV2.

(c) UAV3.

FIGURE 5. GNs' scheduling and transmit power with UAVs. (a) UAV1. (b) UAV2. (c) UAV3.

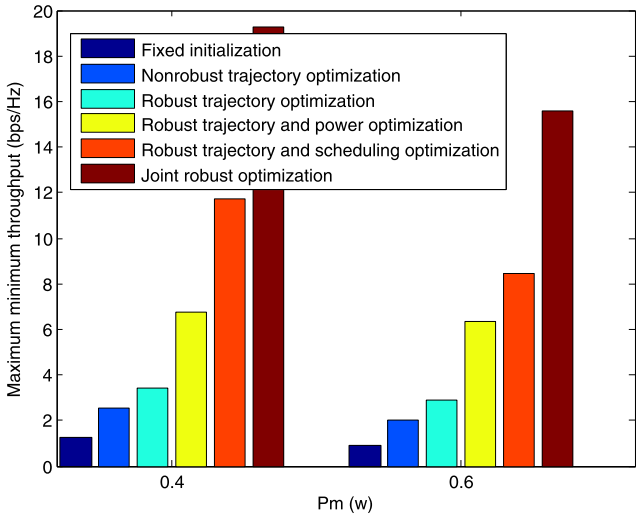

FIGURE 6. The maximum minimum throughput of all GNs of our proposed algorithm and benchmark algorithms.

GNs' scheduling and transmit power allocation. Specifically, the transmit power can be allocated as much as possible to the UAV-GN links in their respective optimal location, for that a intermediate speed is neither optimal for legitimate transmission nor jamming resistance.

In Fig. 5, the details of GNs' scheduling and transmit power allocation for the three UAVs in the "Robust trajectory optimization" are illustrated. It is shown that UAV 1 is associated with GN 1,2,3,5,6, UAV 2 is associated with GN 1,3,4,5,6 and UAV 3 is associated with GN 1 and 3 during the whole time slot. All GNs are allocated with diverse transmit power. This is because the trajectories of UAV 1 and UAV 2 are closer to GNs than UAV 1 at most time slot so that UAV 1 and UAV 2 can serve more GNs to achieve a better system performance. Specifically, combining the observation in 4(c), when UAV 1 and UAV 2 are at the time slots with a relatively low flying speed, the associated GNs allocate maximum transmit power to achieve optimal system performance, which further verifies the scheduling and power allocation design of our proposed "Joint robust optimization".

Two more benchmark algorithms are introduced to evaluate the "Joint robust optimization", i.e., joint robust trajectory and GNs' transmit power optimization with GNs' scheduling set as the "Fixed initialization" (Robust trajectory and power optimization) and joint robust trajectory and GNs' scheduling optimization with GNs' transmit power set as the "Fixed initialization" (Robust trajectory and scheduling optimization). In Fig. 6, the maximum minimum throughput of all GNs of our proposed algorithm "Joint robust optimization" along with benchmark algorithms when $P_m = 0.4$ and $P_m = 0.6$ are illustrated, respectively. It is observed that "Fixed initialization" initialized by intuition is of the lowest efficiency. "Nonrobust trajectory optimization" optimizes the trajectory of UAVs to improve the system performance without handing the uncertain region of jammers, which brings slightly gains. "Robust trajectory optimization" further improves the system performance compared to the "Nonrobust trajectory optimization", which validates the robust design of our proposed algorithm. Particularly, the "Robust trajectory and scheduling optimization" outperforms the "Robust trajectory and power optimization". This is because the optimization of scheduling of GNs is a passive way to optimize the trajectories of UAVs, and the optimization of GNs' transmit power is highly susceptible to the distance between GNs and UAVs, which makes it contributes less to the maximum minimum throughput. However, the joint trajectory, GNs' scheduling and transmit power allocation design outperforms all the benchmark algorithms and enhance the maximum minimum throughput significantly, which further verifies our proposed "Joint robust optimization".

To verify the performance of **Algorithm 2** and compare the system performance of different QoS requirement, we apply **Algorithm 1** and **Algorithm 2** into sub-problems of MAT and MMTD, respectively. Fig. 7 shows the iteration of our proposed algorithms for MMT, MAT and MMTD. It is illustrated that the corresponding algorithms converge to the optimal solution after a number of iterations. Fig. 8 shows each GN's throughput derived by MMT, MAT, and MMTD problems. It can be observed that MAT improves the average throughput of all GNs significantly, but the throughput of GN 3 is much lower than that in MMT. On the contrary, MMT enhances the performance of GN 3 so that the minimum throughput of GNs is higher than that in MAT and performs

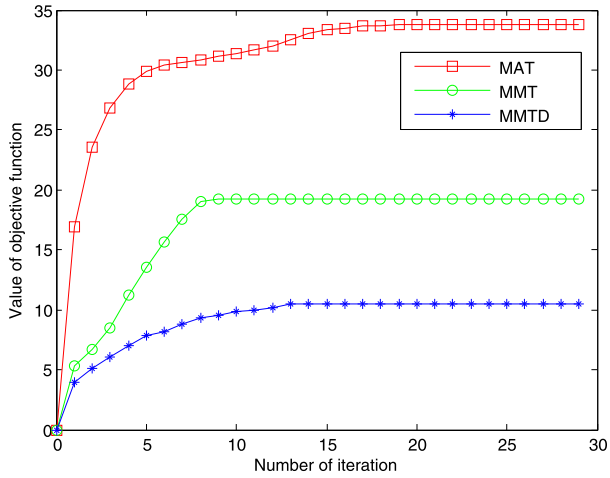

FIGURE 7. The iteration of our proposed algorithms for MAT, MMT and MMTD.

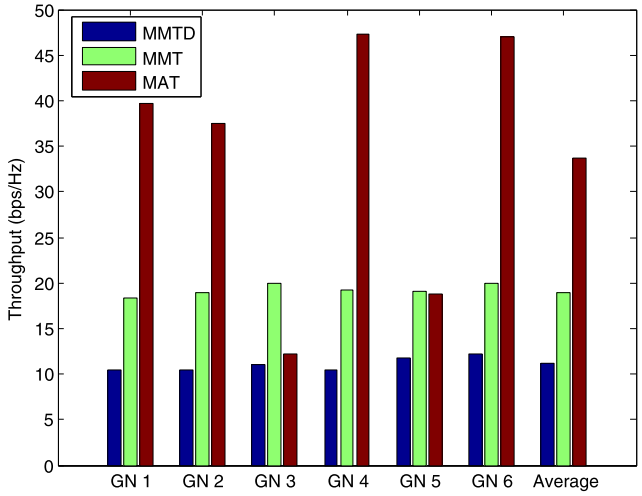

FIGURE 8. System performance of our proposed algorithms for MAT, MMT and MMTD.

ineffectively in enhancing the average throughput of all GNs. However, MAT can reach much better performance both in sum throughput and minimum throughput than MMT if the worst case of GNs, i.e., GN 3, is acceptable. Moreover, to guarantee the delay demand for GN 3, we set $\theta_3 = 0.5$, $\theta_k^{ini} = 1$ and $I_{count} = 20$ in **Algorithm 2** for MMTD. It is illustrated that although the delay constraint of GN 3 is guaranteed, both the average throughput and the minimum throughput of all GNs are decreased, which implies that the delay consideration for the GNs causes large system cost. Hence, **Algorithm 2** is verified. Base on the above discussion, optional algorithms can be provided for diverse applications with specifical QoS requirements, giving a certain practical significance.

VIII. CONCLUSION

In this paper, we investigate a multi-UAV enabled wireless network where the energy constraint GNs are scheduled to transmit information to the UAVs with trajectory properly designed in the 3D space while a number of jammers with uncertain location sending jamming signals. By applying BCD method, SCA technique and $\mathcal{S}$-Procedure, a joint UAVs' trajectory and GNs' scheduling and transmit power allocation optimization algorithm is proposed. Three QoS consideration, i.e., MMT, MAT and MMTD, are proposed to provide guarantees for different applications. Particularly, a parameter aided block coordinate descent method is applied for MMTD problem. Numerical results show that our proposed robust algorithms can significantly improve the corresponding QoS requirement of the multi-UAV enabled wireless networks compared to the benchmark methods.

REFERENCES

[1] Y. Zeng, J. Lyu, and R. Zhang, "Cellular–connected UAV: Potential, challenges, and promising technologies," *IEEE Wireless Commun.*, vol. 26, no. 1, pp. 120–127, Feb. 2019.
[2] Y. Zeng, R. Zhang, and T. J. Lim, "Wireless communications with unmanned aerial vehicles: Opportunities and challenges," *IEEE Commun. Mag.*, vol. 54, no. 5, pp. 36–42, May 2016.
[3] M. Mozaffari, W. Saad, M. Bennis, Y.-H. Nam, and M. Debbah, "A tutorial on UAVs for wireless networks: Applications, challenges, and open problems," *IEEE Commun. Surveys Tuts.*, vol. 21, no. 3, pp. 2334–2360, 3rd Quart., 2019.
[4] H. Wang, G. Ren, J. Chen, G. Ding, and Y. Yang, "Unmanned aerial vehicle-aided communications: Joint transmit power and trajectory optimization," *IEEE Wireless Commun. Lett.*, vol. 7, no. 4, pp. 522–525, Aug. 2018.
[5] Z. Xue, J. Wang, G. Ding, H. Zhou, and Q. Wu, "Maximization of data dissemination in UAV-supported Internet of Things," *IEEE Wireless Commun. Lett.*, vol. 8, no. 1, pp. 185–188, Feb. 2019.
[6] Y. Zeng, R. Zhang, and T. J. Lim, "Throughput maximization for UAV–enabled mobile relaying systems," *IEEE Trans. Commun.*, vol. 64, no. 12, pp. 4983–4996, Dec. 2016.
[7] Y. Zeng and R. Zhang, "Energy–efficient UAV communication with trajectory optimization," *IEEE Trans. Wireless Commun.*, vol. 16, no. 6, pp. 3747–3760, Jun. 2017.
[8] W. Yang, L. Tao, X. Sun, R. Ma, Y. Cai, and T. Zhang, "Secure on–off transmission in mmWave systems with randomly distributed eavesdroppers," *IEEE Access*, vol. 7, pp. 32681–32692, 2019.
[9] X. Sun, W. Yang, Y. Cai, L. Tao, Y. Liu, and Y. Huang, "Secure transmissions in wireless information and power transfer millimeter–wave ultra–dense networks," *IEEE Trans. Inf. Forensics Security*, vol. 14, no. 7, pp. 1817–1829, Jul. 2019.
[10] Z. Xiang, W. Yang, G. Pan, Y. Cai, and Y. Song, "Physical layer security in cognitive radio inspired NOMA network," *IEEE J. Sel. Topics Signal Process.*, vol. 13, no. 3, pp. 700–714, Jun. 2019.
[11] Z. Xiang, W. Yang, G. Pan, Y. Cai, Y. Song, and Y. Zou, "Secure transmission in HARQ–assisted non-orthogonal multiple access networks," *IEEE J. Sel. Topics Signal Process.*, to be published, doi: 10.1109/tifs.2019.2955792.
[12] Z. Xiang, W. Yang, G. Pan, Y. Cai, and X. Sun, "Secure transmission in non–orthogonal multiple access networks with an untrusted relay," *IEEE Wireless Commun. Lett.*, vol. 8, no. 3, pp. 905–908, Jun. 2019.
[13] X. Xu, W. Yang, Y. Cai, and S. Jin, "On the secure spectral–energy efficiency tradeoff in random cognitive radio networks," *IEEE J. Sel. Areas Commun.*, vol. 34, no. 10, pp. 2706–2722, Oct. 2016.
[14] G. Pan, J. Ye, and Z. Ding, "Secure hybrid VLC–RF systems with light energy harvesting," *IEEE Trans. Commun.*, vol. 65, no. 10, pp. 4348–4359, Oct. 2017.
[15] G. Pan, J. Ye, and Z. Ding, "On secure VLC systems with spatially random terminals," *IEEE Commun. Lett.*, vol. 21, no. 3, pp. 492–495, Mar. 2017.
[16] G. Zhang, Q. Wu, M. Cui, and R. Zhang, "Securing UAV communications via joint trajectory and power control," *IEEE Trans. Wireless Commun.*, vol. 18, no. 2, pp. 1376–1389, Feb. 2019.
[17] Y. Cai, F. Cui, Q. Shi, M. Zhao, and G. Y. Li, "Dual-UAV-enabled secure communications: Joint trajectory design and user scheduling," *IEEE J. Sel. Areas Commun.*, vol. 36, no. 9, pp. 1972–1985, Sep. 2018.
[18] F. Cheng, G. Gui, N. Zhao, Y. Chen, J. Tang, and H. Sari, "UAV-relaying-assisted secure transmission with caching," *IEEE Trans. Commun.*, vol. 67, no. 5, pp. 3140–3153, May 2019.

[19] Q. Wang, Z. Chen, and H. Li, "Energy-efficient trajectory planning for UAV-aided secure communication," *China Commun.*, vol. 15, no. 5, pp. 51–60, May 2018.
[20] L. Xiao, Y. Xu, D. Yang, and Y. Zeng, "Secrecy energy efficiency maximization for UAV–enabled mobile relaying," *IEEE Trans. Green Commun. Netw.*, to be published, doi: 10.1109/tgcn.2019.2949802.
[21] C. Zhong, J. Yao, and J. Xu, "Secure UAV communication with cooperative jamming and trajectory control," *IEEE Commun. Lett.*, vol. 23, no. 2, pp. 286–289, Feb. 2019.
[22] X. Sun, C. Shen, D. W. K. Ng, and Z. Zhong, "Robust trajectory and resource allocation design for secure UAV–aided communications," in *Proc. IEEE ICC Workshops*, May 2018, pp. 1–6.
[23] M. Cui, G. Zhang, Q. Wu, and D. W. K. Ng, "Robust trajectory and transmit power design for secure UAV communications," *IEEE Trans. Veh. Technol.*, vol. 67, no. 9, pp. 9042–9046, Sep. 2018.
[24] Y. Cai, Z. Wei, R. Li, D. W. Kwan Ng, and J. Yuan, "Energy–efficient resource allocation for secure UAV communication systems," in *Proc. IEEE WCNC*, Apr. 2019, pp. 1–8.
[25] L. Xiao, C. Xie, M. Min, and W. Zhuang, "User–centric view of unmanned aerial vehicle transmission against smart attacks," *IEEE Trans. Veh. Technol.*, vol. 67, no. 4, pp. 3420–3430, Apr. 2018.
[26] Y. Xu, G. Ren, J. Chen, Y. Luo, L. Jia, X. Liu, Y. Yang, and Y. Xu, "A one-leader multi-follower Bayesian–Stackelberg game for anti-jamming transmission in UAV communication networks," *IEEE Access*, vol. 6, pp. 21697–21709, 2018.
[27] H. Wang, J. Chen, G. Ding, and J. Sun, "Trajectory planning in UAV communication with jamming," in *Proc. 10th Int. Conf. Wireless Commun. Signal Process. (WCSP)*, Oct. 2018, pp. 1–6.
[28] M.-C. Mah, H.-S. Lim, and A. W.-C. Tan, "UAV relay flight path planning in the presence of jamming signal," *IEEE Access*, vol. 7, pp. 40913–40924, 2019.
[29] H. Wang, J. Wang, G. Ding, J. Chen, Y. Li, and Z. Han, "Spectrum sharing planning for full-duplex UAV relaying systems with underlaid D2D communications," *IEEE J. Sel. Areas Commun.*, vol. 36, no. 9, pp. 1986–1999, Sep. 2018.
[30] B. Duan, D. Yin, Y. Cong, H. Zhou, X. Xiang, and L. Shen, "Anti-jamming path planning for unmanned aerial vehicles with imperfect jammer information," in *Proc. IEEE ROBIO*, Dec. 2018, pp. 729–735.
[31] Q. Wu, Y. Zeng, and R. Zhang, "Joint trajectory and communication design for multi-UAV enabled wireless networks," *IEEE Trans. Wireless Commun.*, vol. 17, no. 3, pp. 2109–2121, Mar. 2018.
[32] H. Wang, J. Wang, G. Ding, J. Chen, F. Gao, and Z. Han, "Completion time minimization with path planning for fixed-wing UAV communications," *IEEE Trans. Wireless Commun.*, vol. 18, no. 7, pp. 3485–3499, Jul. 2019.
[33] Q. Wu and R. Zhang, "Common throughput maximization in UAV-enabled OFDMA systems with delay consideration," *IEEE Trans. Commun.*, vol. 66, no. 12, pp. 6614–6627, Dec. 2018.
[34] Y. Xu, L. Xiao, D. Yang, Q. Wu, and L. Cuthbert, "Throughput maximization in multi-UAV enabled communication systems with difference consideration," *IEEE Access*, vol. 6, pp. 55291–55301, 2018.
[35] D. Tse and P. Viswanath, *Fundamentals of Wireless Communication*. Cambridge, U.K.: Cambridge Univ. Press, 2005.
[36] M. Grant and S. Boyd. *CVX: MATLAB Software for Disciplined Convex Programming*. Accessed: Mar. 2016. [Online]. Available: https://cvxr.com/cvx
[37] S. Boyd and L. Vandenberghe, *Convex Optimization*. Cambridge, U.K.: Cambridge Univ. Press, 2004.

YANG WU received the B.S. and M.S. degrees from the PLA University of Science and Technology, in 2012 and 2015, respectively. He is currently pursuing the Ph.D. degree in cyberspace security with the Institute of Communications Engineering, Army Engineering University of PLA. His research interests include physical layer security, UAV communication, and convex optimization.

WENLU FAN received the B.S. degree in statistics from the Mathematics Department, Nanjing University, Nanjing, China, in 2019, where she is currently pursuing the M.S. degree in international trade with the Business School. Her current research interests include UAV communication and data analysis.

WEIWEI YANG received the B.Sc., M.Sc., and Ph.D. degrees in telecommunications from the PLA University of Science and Technology, Nanjing, China, in 2003, 2006, and 2011, respectively. He is currently an Associate Professor with the College of Communication Engineering, Army Engineering University of PLA. He has coauthored the book *Handbook of Cognitive Radio* (Springer, 2017). His research interests include cooperative communications, cognitive radio, and physical layer security. He was a co-recipient of the Best Paper Award from WCSP 2011. He served as the Publication Co-Chair for WCSP 2015, the Track Chair for the IEEE CIC ICCC 2017 and WCSP 2015, and a TPC Member for WCSP 2011/2014/2017/2018, GC 2016 Workshops, GC 2017 Workshops, and ICC 2016 Workshops.

XIAOLI SUN received the B.S. and M.S. degrees from the PLA University of Science and Technology, in 2014 and 2017, respectively. She is currently pursuing the Ph.D. degree in communications and information system with the Institute of Communications Engineering, Army Engineering University of PLA. Her research interests include physical layer security, relaying networks, millimeter-wave communication, and UAV communication.

XINRONG GUAN received the B.S. degree in communications engineering and the Ph.D. degree in communications and information systems from the Institute of Communications Engineering, PLA University of Science and Technology, Nanjing, China, in 2009 and 2014, respectively. His current research interests include physical layer security, wireless key generation, cooperative communications, and cognitive radio networks.